






CLASSIFICATION OF THE SPECTRAL FINE STRUCTURE IN AURORAL KILOMETRIC RADIATION

U. Taubenschuss¹ , G. Fischer² , D. Píša¹ ,
O. Santolík^{1,3} , and J. Souček¹ 

*Corresponding author: ut@ufa.cas.cz

Citation:

Taubenschuss et al., 2023, Classification of the spectral fine structure in Auroral Kilometric Radiation, *in Planetary, Solar and Heliospheric Radio Emissions IX*, edited by C. K. Louis, C. M. Jackman, G. Fischer, A. H. Sulaiman, P. Zucca, published by DIAS, TCD, pp. 139–151, doi: 10.25546/103089

Abstract

Auroral Kilometric Radiation (AKR) is generated by unstable energetic electron populations in the auroral region of Earth’s magnetosphere. A mechanism known as the cyclotron maser instability amplifies weak background radiation at the expense of particle energy. However, this instability alone can not explain frequent observations of AKR spectral fine structures when recorded with sufficiently high time and frequency resolution. We will analyse observations of AKR from the Cluster Wideband Receiver and give an overview of the different types of spectral fine structures found in this dataset for the years 2002 and 2003. A classification scheme is introduced, and the occurrence rate for each class of fine structure is investigated in a statistical analysis. Finally, possible generation mechanisms will be discussed in relation to the observations.

¹ *Institute of Atmospheric Physics, Czech Academy of Sciences, Prague, Czechia*

² *Space Research Institute, Austrian Academy of Sciences, Graz, Austria*

³ *Faculty of Mathematics and Physics, Charles University, Prague, Czechia*

1 Introduction

A dynamic interaction between electric fields and energetic particles in the auroral region of Earth's magnetosphere creates favorable conditions for the generation of powerful radio emissions, the so-called Auroral Kilometric Radiation (AKR) (Benediktov et al., 1965; Gurnett, 1974). Observed AKR frequencies are inside a range of 30 - 1000 kHz (Hanasz et al., 1998) suggesting sources at radial distances of $1.2 - 3.7 R_E$ ($1 R_E = 6371$ km), based on a simple dipole model for Earth's magnetic field. AKR sources are distributed along high-latitude magnetic field lines that connect to the auroral oval (L-shell ~ 10). This region features strong parallel electric fields and a geometry of converging magnetic field lines where electron distributions at 1 - 10 keV energy become modified and eventually unstable to direct amplification of X-mode and O-mode radio waves at the local electron cyclotron frequency f_c . This mechanism is known as the cyclotron maser instability (CMI) which was found to operate on the basis of a loss-cone distribution for magnetospherically reflected electrons (Wu & Lee, 1979) and, more efficiently, on the basis of a partial shell or horseshoe distribution for the descending electron population (Pritchett, 1984; Ergun et al., 2000). The X-mode can grow inside density cavities where $0.02 < f_p/f_c < 0.2$ (Melrose et al., 1984). Here, f_p indicates the electron plasma frequency. Weaker O-mode AKR is observed at intensities of 10 - 20 dB below that of the X-mode (Mellott et al., 1984; Mutel et al., 2007). It is yet unclear if the O-mode is directly amplified through the CMI as well (in regions outside of the density cavities, where $f_p/f_c > 0.3$) or if it is a by-product from X-mode reflections at strong density gradients in the cavity's boundary (Hayes & Melrose, 1986). Observations of spectral fine structures in O-mode AKR (Benson et al., 1988) support both mechanisms. Wave propagation analysis indicates at least different source regions for simultaneously observed X-mode and O-mode AKR (Santolík & Parrot, 2006).

Remote and in-situ observations from spacecraft reveal a complex spectral fine structure for AKR which consists of narrowband emission that is drifting up and down in frequency on time scales of milliseconds to minutes (Gurnett et al., 1979; Grabbe, 1982; Benson et al., 1988; Oya et al., 1990; Menietti et al., 1996; Hanasz et al., 1998; Pottellette et al., 2001; Mutel et al., 2006; Su et al., 2008). This indicates that auroral particle acceleration is a highly dynamical process, and that the CMI alone is insufficient to describe the complex relation between modifications of particle distributions, shifts in source altitude and electromagnetic wave amplification. Many different theories for a production of AKR spectral fine structure have been proposed over the past fifty years. We will refrain from summarizing each and every one of these theories, but will instead comment briefly in Section 4 on those which seem to be relevant for the fine structures found in this study. The data used here from the Cluster mission are described in Section 2. Seven major classes of AKR spectral fine structures are drafted in Section 3, including several spectrograms as representative examples. Finally, our results are discussed in Section 4.

Table 1: Volume of Cluster Wideband data included in this study, separated into the four possible frequency bands of observation (marked by nominal bandpass range; first column). The cadence of waveform snapshots in the baseband is 79.4 ms. For the downconverted bands in continuous mode, a window length of 1024 samples, where neighboring windows overlap by 50%, results in a time resolution of $\Delta t = 18.6$ ms. Δf indicates the frequency resolution. The last column is listing the fraction of time for which AKR is visible in each band. Data are from Jan - Nov, 2002, and from Feb - Dec, 2003. On average, AKR is observed for $\sim 65\%$ of the time across all four bands.

Obs. Band [kHz]	Δt [ms]	Δf [Hz]	No. Inspect. Spectra	Inspect. Time [h]	Showing AKR [%]
0 - 77	79.4	107.2	14815	221.2	48.8
125 - 134.5	18.6	26.8	9179	81.6	75.8
250 - 259.5	18.6	26.8	12751	115.0	87.6
500 - 509.5	18.6	26.8	9239	81.8	65.6

2 Instruments and data processing

The Cluster mission consists of four satellites, each carrying an identical set of instruments for measuring plasma parameters and electromagnetic waves in near-Earth space. We will use data from the Cluster Wideband Receiver (WBD) (Gurnett et al., 1997) which is connected to the Electric Field and Wave (EFW) instrument (Gustafsson et al., 1997), receiving signals from one of two electric wire antennas. Magnetic signals can not be included because of instrumental limitations to a frequency range below that of AKR. Since the input to the WBD is limited to a single antenna at a time, polarisation analysis is not possible. Consequently, the spectral fine structure of AKR will be displayed only in terms of electric power spectral density.

For AKR observations, WBD is used in two operational modes: a *continuous* mode that samples the electric waveform up to several minutes at 27.4 kHz sampling rate, and a *snapshot* mode that provides higher sampling rates of either 54.9 kHz (rarely used) or 219.5 kHz, but which is duty cycled, so that snapshots of 2180 samples are taken every 79.4 ms. Thus, sub-second spectral fine structure is only classifiable with continuous mode data. Both modes can be operated in the baseband (starting at <1 kHz) or they can be downconverted from higher starting frequencies at 125 kHz, 250 kHz and 500 kHz. All four bands are used in a cyclic fashion to cover the frequency range of AKR.

An overview of the investigated volume of data is given in Table 1. Each spectrogram in our catalogue has a duration of 36 s in continuous-mode and 1 minute in snapshot-mode. If a certain fine structure is found in a spectrogram, this is counted as an event. One spectrogram can contain many different types of fine structures which all add to their individual count rates. Since the continuous-mode together with downconversion was mainly used at the beginning of the Cluster mission, and since during the later years several electrical probes failed, we concentrated our search on the earlier years 2002 and 2003. In total, almost 46 000 WBD spectrograms have been manually inspected for AKR fine structure.

3 Classes of AKR spectral fine structures

We present seven major types of AKR spectral fine structures that are regularly observed with Cluster-WBD during the years 2002 and 2003. The spectral characteristics of each

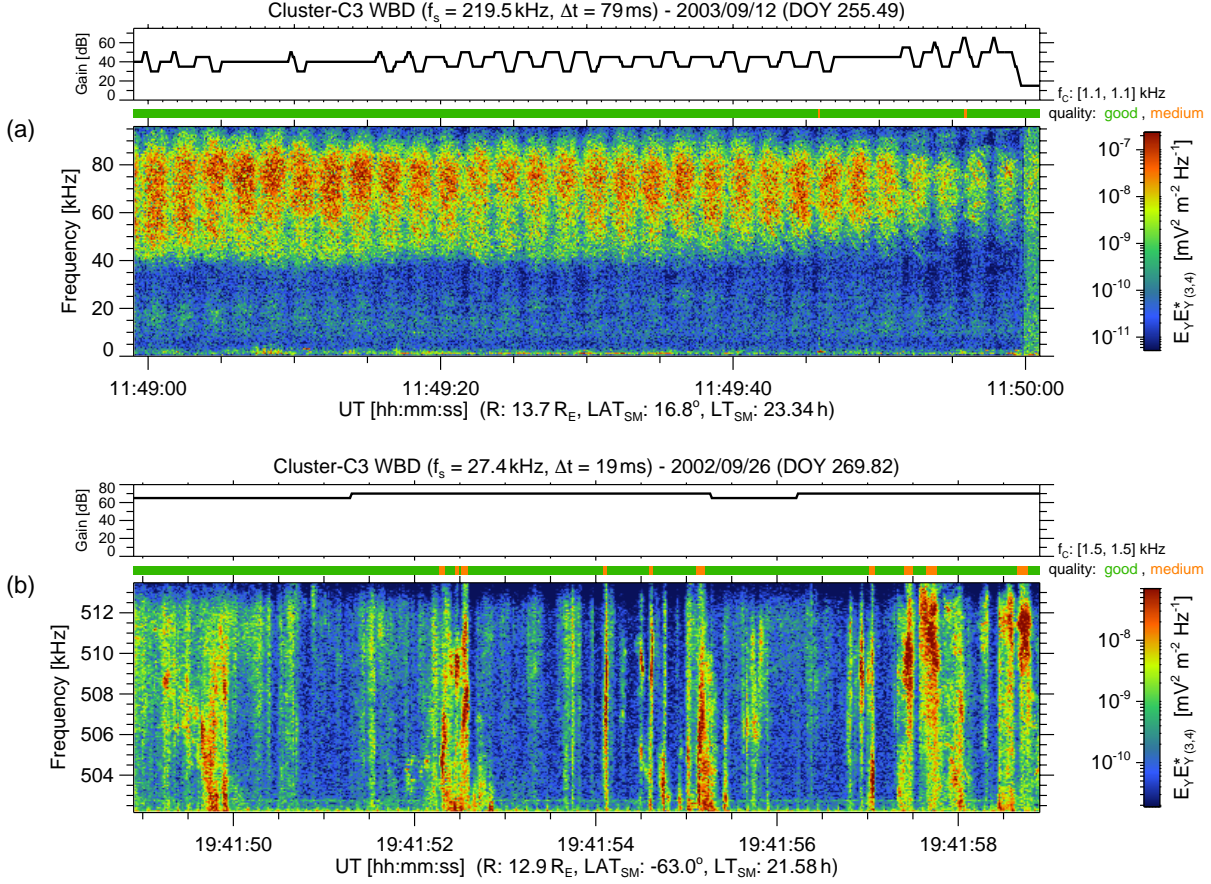


Figure 1: Cluster WBD spectrograms of (a) spin-modulated Diffuse AKR from the baseband (snapshot mode; ~ 1 minute of data displayed) and (b) AKR Vertical Lines as observed in the highest downconverted band (continuous mode; ~ 10 seconds of data displayed). Dimming of emission near the upper frequency boundary is due to filtering. Both panels include a Gain-profile and a bar indicating data quality on top. Besides time, average spacecraft solar-magnetic (SM) coordinates are listed below the x-axis in terms of radial distance (R), magnetic latitude (LAT) and magnetic local time (LT).

type are described on the basis of a representative spectrogram. This classification scheme is similar to the one of Fischer et al. (2022) which was introduced for Saturn Kilometric Radiation.

3.1 Diffuse AKR and vertical lines

We start with a class named *Diffuse AKR*, which actually contains no fine structure at all. This type is characterised by broadband (>10 kHz bandwidth) and continuous emission over many seconds to minutes. An example is shown in Figure 1a from the baseband, where diffuse emission is covering a frequency range between 40 kHz and ~ 90 kHz. The latter is the visible upper cutoff of the WBD bandpass filter. The only modulations visible are sinusoidal variations of intensity as a function of time which are due to a changing angle of incidence of the wave vector with respect to the E_y -antenna in the course of the spacecraft's spin (~ 4 s spin period). Thus, intensity minima are separated by ~ 2 s (half spin period). Diffuse AKR is also often observed in the downconverted bands, at

frequencies >100 kHz, where the WBD bandwidth is more limited. For these cases, we demand smooth emission across the entire observable frequency range of approximately 11 kHz (nominal 9.5 kHz). It should be noted that some of these events may belong to type III solar radio bursts, which are sometimes present below 500 kHz, and which would leave a diffuse spectral signature as well.

Figure 1b shows an example of discrete features in AKR which are recognized as a structuring of emission into thin vertical lines; thus the name *AKR Vertical Lines*. The gain profile (see top of Figure 1b) confirms that these lines are not caused by synchronous switches in instrumental gain. A specific example of this is seen in Figure 1a at 11:50:00 UT, where the background intensity is elevated across the entire frequency range due to a drop in gain. In order to be classified as AKR Vertical Lines, we demand a temporal width <1 s per line, and a vertical extent of >10 kHz. It remains unclear if these structures are indeed vertical in the spectrogram or if they just happen to have a frequency drift rate that exceeds the maximum resolvable drift after FFT, which is approximately 600 kHz s^{-1} ($\sim 11 \text{ kHz}/18.6 \text{ ms}$).

3.2 AKR striations

AKR Striations are seen in spectrograms as narrowband (<1 kHz) line-like emissions that drift in frequency over time (Menietti et al., 1996). Drift rates range from a few kHz s^{-1} to a few tens of kHz s^{-1} , and they can be positive or negative. Maximum durations are in the order of 5 - 10 s. Two examples of striations are presented in Figure 2. Panel (a) shows more irregularly drifting positive striations, and panel (b) contains a dense group of negatively drifting striations. In fact, a linear drift is rarely observed for positive striations, in contrast to the negative ones. Another feature that characterises striations is their occurrence in groups, with a rapid cadence of successive single lines, all exhibiting very similar drift rates, as shown in Figure 2b. On rare occasions, spectrograms may contain two overlapping groups of striations, each exhibiting a significantly different drift, probably belonging to different AKR source regions.

3.3 AKR rain and bursts

Often, AKR Striations seem to be chopped into shorter segments, with individual segments slightly displaced in time so that they can not be connected to a longer drifting structure anymore. Such cases form a separate class called *AKR Rain*, a term which was first introduced by Mutel et al. (2004). Individual elements of AKR Rain usually last for <1 s, and they are often irregularly shaped in a spectrogram, but they do follow a common average drift rate when observed over several seconds. Three examples for AKR Rain are shown in Figure 3 for (a) negative drift, (b) positive drift and (c) \sim zero average drift. The last group is defined by no drift on average, meaning that individual elements can drift very slowly ($< 1 \text{ kHz s}^{-1}$) in a negative or positive sense. Such slow drift rates are not observed for striations, which suggests that non-drifting Rain is not necessarily resulting directly from interrupted striations.

One can also consider single elements of AKR Rain as *AKR Bursts*. The latter class

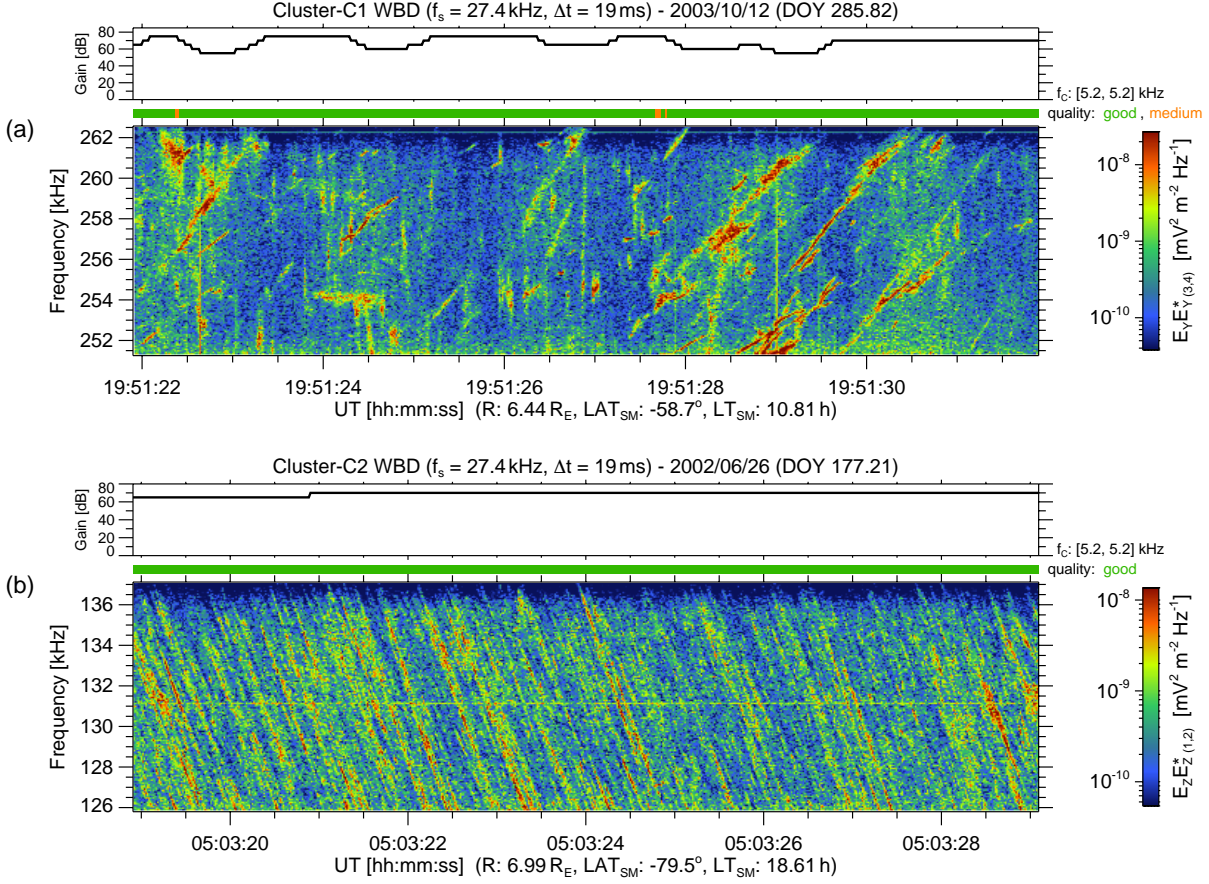


Figure 2: Examples of AKR Striations with (a) positive drift rates (approx. $+6.0 \text{ kHz s}^{-1}$) and (b) negative drift rates (approx. -12.6 kHz s^{-1}). Both panels display ~ 10 seconds of data. Negative striations are denser and more regular than positive ones.

is introduced for short elements occurring sporadically, comparable to sporadic drops of rain. We have no exact definition for a threshold between these two classes, e.g. a certain burst-count per second classifies as Rain, given that the transition is fluent anyway. However, we shall follow a loose initial separation into AKR Bursts and Rain for statistical reasons, to verify that Bursts occurring as single events are rather uncommon, and that they rather tend to group as Rain (see also Figure 5).

It should be noted that these two classes can only be identified reliably in the downconverted bands, which provide enough spectral resolution. Since individual elements of Rain and Bursts are shorter than 2 s, they are usually not affected by intensity modulations due to the spacecraft's spin. Anyhow, we ensured to disregard spectral features that appear bursty but are actually artifacts of regular spin modulations.

3.4 AKR bands and snakes

AKR is frequently observed in the form of banded emissions that can drift up and down in frequency. Two classes are introduced for separating between regularly and irregularly drifting bands. An example of the former, so-called *AKR Bands*, is shown in Figure 4a, where all six visible AKR Bands exhibit a positive drift rate. AKR Bands are characterised

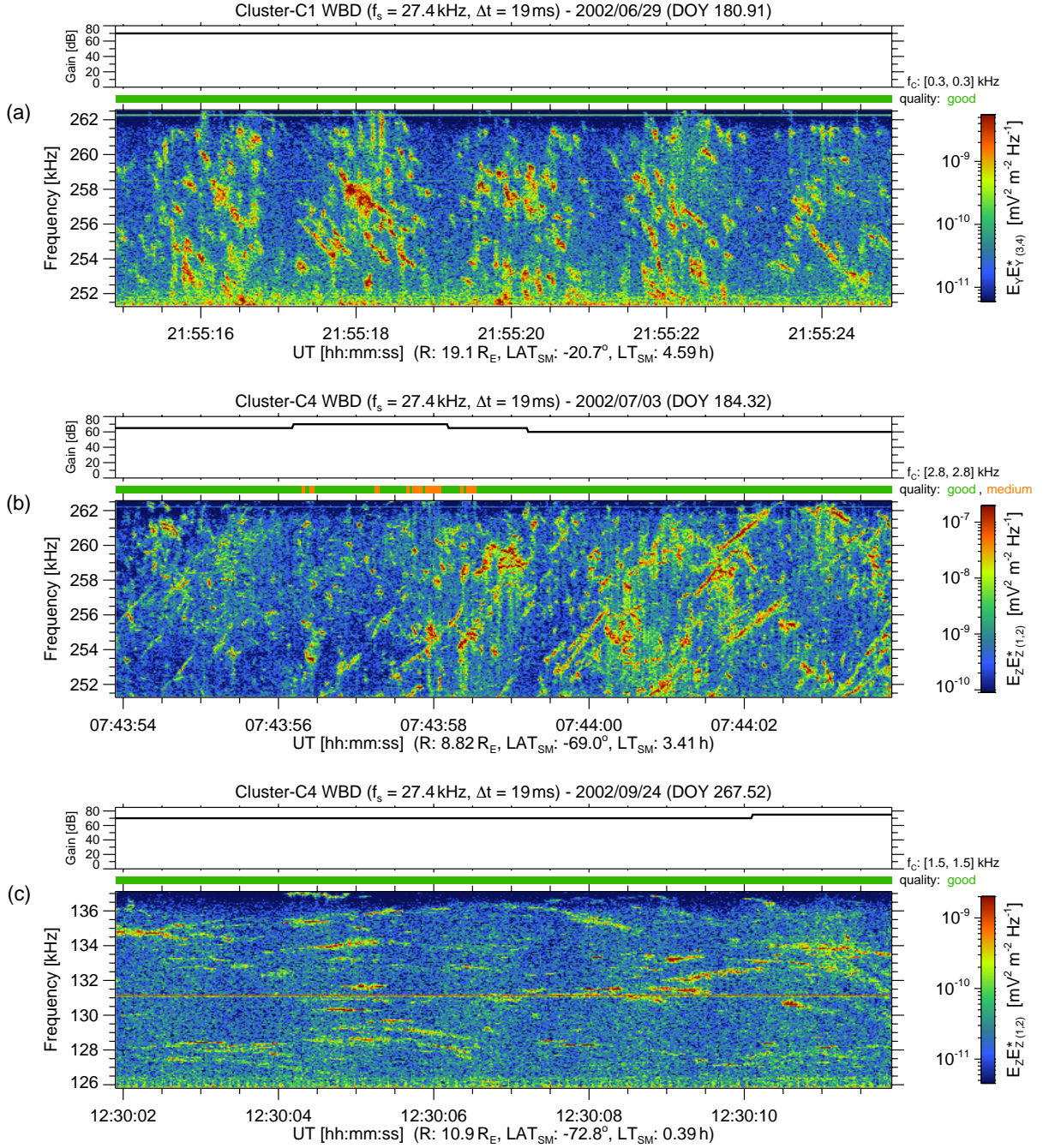


Figure 3: AKR Rain with (a) negative drift (approx. -5.1 kHz s⁻¹), (b) positive drift (approx. $4.2 - 6.6$ kHz s⁻¹) and (c) \sim zero average drift. All three panels display ~ 10 seconds of data.

by a bandwidth of < 2 kHz, slow absolute drift rates of < 1 kHz s⁻¹ and relatively little or unclear sub-structuring within a band. The emission can be seen monotonically rising or falling in frequency for durations of minutes.

In contrast, irregular bands exhibit a more chaotic spectral behavior with rapid excursions up and down in frequency. An example is shown in Figure 4b. This class is named *AKR Snakes* due to their wavy spectral pattern. The bandwidth is limited to < 2 kHz as well, but Snakes do often contain visible sub-structure in the form of narrowband bursts (usually

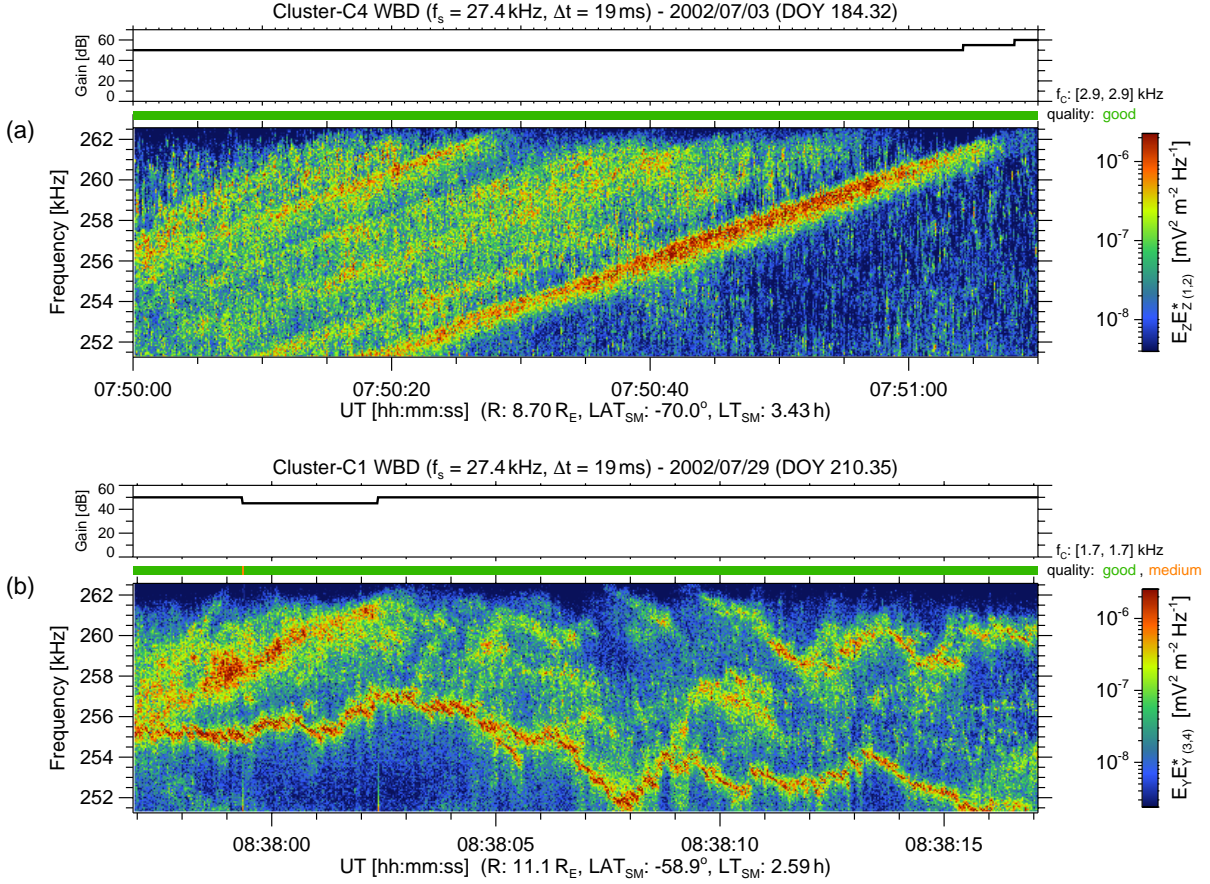


Figure 4: (a) AKR Bands with a positive drift rate ($\sim 0.22 \text{ kHz s}^{-1}$; ~ 80 seconds displayed) and (b) irregularly drifting AKR Snakes (~ 20 seconds displayed). The emission in (a) below the intensive bottom Band is AKR Rain (unresolved).

negatively drifting). Moreover, Snakes are frequently interrupted and can perform step-like jumps in frequency across several kHz. Another peculiarity of Snakes are associated dropouts of emission just below a Snake, which is best visible when Snakes occur together with Diffuse AKR. Such a feature might be present in Figure 4b between 08:38:00 - 08:38:05 UT, where the Snake near 256 kHz seems to outline a boundary between AKR emission above and an absence of emission below.

4 Results and discussion

Seven major types of AKR spectral fine structures frequently seen in Cluster-WBD spectrograms have been presented in Section 3. Besides the already documented AKR Striations and Rain (Menietti et al., 1996; Mutel et al., 2004), we introduce five additional classes: Diffuse AKR, Vertical Lines, Bursts, Bands and Snakes. This classification is solely based on spectral characteristics. All other kinds of fine structures are marked as *Irregular* AKR in our catalogue. Irregular emissions are not distinct and repetitive enough to justify another separate class.

The occurrence probabilities for all seven classes are summarized in Figure 5. Occurrence

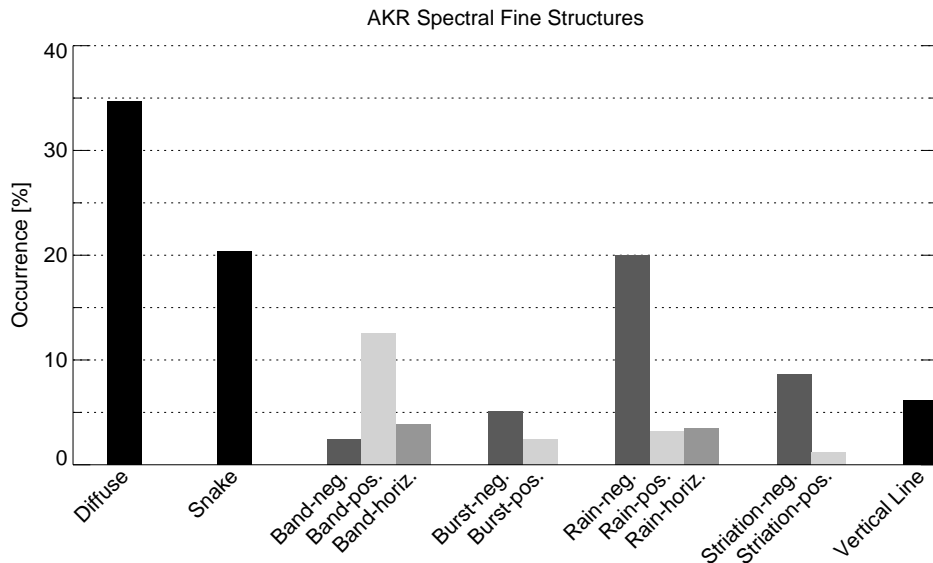


Figure 5: Occurrence statistics for the seven standard classes of AKR spectral fine structure as observed by Cluster/WBD during the years 2002 and 2003. Occurrence is defined as the percentage of time for which a certain class is visible. Some classes are divided into negatively and positively drifting subclasses. Bands and Rain have an additional subclass for \sim zero drift (horiz.).

is defined as the fraction of time during which a certain class is visible. Spectrograms without any AKR are excluded from the statistics, based on the fact that WBD data streams are discontinuous anyway (WBD active for a few hours per day only).

Diffuse AKR: Diffuse AKR is by far the most common type of spectral structure with an occurrence close to 35%. A generation of diffuse emission across a broad frequency range (>10 kHz) is difficult to explain in terms of the CMI which is a narrowbanded mechanism by nature. X-mode growth based on a shell or horseshoe distribution is expected to have a $\Delta f/f < 0.01$ (Ergun et al., 2000; Mutel et al., 2011). However, it is plausible that several adjacent AKR sources are simultaneously active along a larger altitude range, each emitting a narrow range of frequencies around the local f_c . During propagation from the source to a distant observer, those parts get mixed, and if emitted radio powers are comparable they inevitably merge to a more uniform broadband spectrum.

Besides Diffuse AKR, all other classes can be roughly divided into coarser structures lasting up to a few minutes, comprising Snakes and Bands, and into finer structures comprising the Striations, Rain, Bursts and Vertical Lines. Bands have a slow (<1 kHz s $^{-1}$) and predominantly positive drift in frequency, whereas all finer structures (except Vertical Lines) have a fast (>1 kHz s $^{-1}$) and predominantly negative drift. This suggests fundamental differences in the generation mechanisms of coarser and finer spectral features.

Striations: An 8.7% occurrence rate for negative striations (Figure 5) is close to the 6% reported by Menietti et al. (2000). Since drift rates correlate well with typical parallel velocities of ion beams and ion acoustic waves in the auroral upward current region (Gurnett & Anderson, 1981; Bounds et al., 1999), it was postulated that electrostatic solitary waves (ESWs) in the form of ion holes may play a significant role (Mutel et al., 2006). An additional electric field of a few 100 mV m $^{-1}$ from an ion hole might be able to reshape

the local electron distribution function and to boost narrowband amplification of X-mode radiation at the local f_c Mutel et al. (2007).

AKR Rain and Bursts: These two spectral features might simply be interrupted AKR Striations, considering that their drift rates are in a similar range as for the striations, and that the common dominant drift is negative. So, a production of Rain and Bursts could be traced back to ion hole interaction as well, although under less favorable conditions. Based on the observations, such ion holes would have lifetimes of < 1 s. These short-lived ion holes seem to be the norm inside an AKR source region given the higher occurrence rate of negative Rain (20%) in comparison to negative striations (8.7%; see Figure 5). Although ESWs have been observed many times in or near the AKR source region (Ergun et al., 1998; Bounds et al., 1999), direct estimates of their lifetimes from multi-spacecraft observations are still pending.

Vertical Lines: Vertical Lines have a rare occurrence of 6.1% (Figure 5), and most are seen in the maximum-frequency observational band starting at 500 kHz. It remains unclear if these structures are indeed vertical or if their spectral drift rate exceeds the maximum resolvable drift (~ 600 kHz s $^{-1}$). Such high drift rates can be provided by electron holes (Ergun et al., 1998) moving downward at parallel speeds of $v > 4000$ km s $^{-1}$ at a 500-kHz source, and $v > 30\,000$ km s $^{-1}$ at a 125-kHz source (dipole field model with $L = 10$). In case of electron hole interaction inside the AKR source region (upward current region), the true drift of “Vertical” Lines should be positive. Fast positively drifting or \sim vertical features in AKR have also been reported by Hanasz et al. (2008), and explained by an interaction of the auroral electron distribution with shear Alfvén waves that propagate at speeds of several 1000 km/s towards the ionosphere. In this scenario, a constant repetition rate for Vertical Lines should be observed that matches the typical frequencies of Pc1 geomagnetic pulsations (1 - 4 Hz).

AKR Bands: AKR Bands exhibit slow drift rates at < 1 kHz s $^{-1}$ and a dominant occurrence of positive drifts (12.6%). The slow drift excludes possible stimulators like electron holes and ion holes, but also EMIC waves (Menietti et al., 1996) and Alfvén waves (Hanasz et al., 2008). Here, we propose that source regions of AKR Bands are located in the vicinity of electrostatic double layers (Block, 1972; Ergun et al., 2004), as has already been suggested in one of the earliest reports about AKR by Gurnett et al. (1979). A double layer is a more stable and large-scale electrostatic structure inside the AKR source region, which may move slowly up and down along the field lines, and which provides a strong electric field to modify the local electron distribution function.

AKR Snakes: As can be seen from Figure 5, Snakes are a very common type of fine structure with an occurrence of 20.4%. It would be simple and convenient to relate an excitation of Snakes to electrostatic double layers as well, and to explain a more chaotic spectral drift and frequent interruptions with more unstable conditions for the associated double layers. However, such spectral characteristics for AKR are also predicted by an early theory published by Calvert (1982), which works on the principle of oscillatory amplification of the X-mode inside density enhancements. Calvert (1982) outlines several characteristics of such an oscillator and its radio emissions: (a) small but rapid fluctuations in oscillator frequency due to fluctuating conditions given at the reflecting boundaries of the density enhancement, (b) interruptions and step-like jumps in frequency due to a shift

of optimum oscillator conditions from one source altitude to another, (c) relatively stable emitted spectral power over time due to oscillator operation at its given saturation level, and (d) similar behavior (spectral drift) of narrowband emissions (Snakes) at neighboring frequencies due to multiple oscillators operating simultaneously at closely spaced altitudes (emission of “multiplets”). A more detailed analysis of Snakes is beyond the scope of this paper, as well as verifying small-scale density enhancements with Cluster, which is in principle possible. However, the existence of an “auroral oscillator” is intriguing, adding new aspects to the interpretation of AKR spectral fine structure.

This work represents a first step towards a classification scheme trying to establish some order among the diverse range of AKR spectral fine structures. Initial statistical results show clear evidence for a variable importance of the seven found classes and their associated generation mechanisms. Some of these mechanisms have been studied to a certain extent, like the influence of phase space holes on AKR Striations, but for others, the underlying physics is still unclear or yet unexplored.

Acknowledgements

The extensive archive of Cluster Wideband data is made accessible through the University of Iowa and the Cluster Science Archive. All authors acknowledge support from the FWF-GAČR international project “Analysis of fine structures in auroral radio emissions” under grant numbers I 4559-N and 20-06802L.

References

- Benediktov E. A., Getmantsev G. G., Sazonov Y. A., Tarasov A. F., 1965, Preliminary results of measurements of the intensity of distributed extraterrestrial radio-frequency emission at 725 and 1525-kHz frequencies by the satellite elektron-2, *Kosmicheskie Issledovaniya*, 3, 614
- Benson R. F., Mellott M. M., Huff R. L., Gurnett D. A., 1988, Ordinary mode auroral kilometric radiation fine structure observed by DE 1, *Journal of Geophysical Research*, 93, 7515
- Block L. P., 1972, Potential double layers in the ionosphere, *Cosmic Electrodynamics*, 3, 349
- Bounds S. R., Pfaff R. F., Knowlton S. F., Mozer F. S., Temerin M. A., Kletzing C. A., 1999, Solitary potential structures associated with ion and electron beams near $1R_E$ altitude, *Journal of Geophysical Research*, 104, 28709
- Calvert W., 1982, A feedback model for the source of auroral kilometric radiation, *Journal of Geophysical Research*, 87, 8199
- Ergun R. E., et al., 1998, FAST satellite observations of large-amplitude solitary structures, *Geophysical Research Letters*, 25, 2041

- Ergun R. E., Carlson C. W., McFadden J. P., Delory G. T., Strangeway R. J., Pritchett P. L., 2000, Electron-cyclotron maser driven by charged-particle acceleration from magnetic field-aligned electric fields, *The Astrophysical Journal*, 538, 456
- Ergun R. E., et al., 2004, Auroral particle acceleration by strong double layers: The upward current region, *Journal of Geophysical Research*, 109, A12220
- Fischer G., Taubenschuss U., Piša D., 2022, Classification of spectral fine structures of Saturn kilometric radiation, *Annales Geophysicae*, 40, 485
- Grabbe C. L., 1982, Theory of the fine structure of auroral kilometric radiation, *Geophysical Research Letters*, 9, 155
- Gurnett D. A., 1974, The Earth as a radio source: Terrestrial kilometric radiation, *Journal of Geophysical Research*, 79, 4227
- Gurnett D. A., Anderson R. R., 1981, The kilometric radio emission spectrum - Relationship to auroral acceleration processes, in *Physics of Auroral Arc Formation*, pp 341–350
- Gurnett D. A., Anderson R. R., Scarf F. L., Fredricks R. W., Smith E. J., 1979, Initial results from the ISEE-1 and -2 Plasma Wave Investigation, *Space Science Reviews*, 23, 103
- Gurnett D. A., Huff R. L., Kirchner D. L., 1997, The Wide-Band plasma wave investigation, *Space Science Reviews*, 79, 195
- Gustafsson G., et al., 1997, The Electric Field and Wave experiment for the Cluster mission, *Space Science Reviews*, 79, 137
- Hanasz J., Schreiber R., de Feraudy H., Mogilevsky M. M., Romantsova T. V., 1998, Observations of the upper frequency cutoffs of the auroral kilometric radiation, *Annales Geophysicae*, 16, 1097
- Hanasz J., Schreiber R., Pickett J., de Feraudy H., 2008, Pulsations of auroral kilometric radiation at Pc1 frequencies, *Geophysical Research Letters*, 35, L15819
- Hayes L. M., Melrose D. B., 1986, Generation of ordinary mode auroral kilometric radiation from extraordinary mode waves, *Journal of Geophysical Research*, 91, 211
- Mellott M. M., Calvert W., Huff R. L., Gurnett D. A., Shawhan S. D., 1984, DE-1 observations of ordinary mode and extraordinary mode auroral kilometric radiation, *Geophysical Research Letters*, 11, 1188
- Melrose D. B., Hewitt R. G., Dulk G. A., 1984, Electron-cyclotron maser emission: Relative growth and damping rates for different modes and harmonics, *Journal of Geophysical Research*, 89, 897
- Menietti J. D., Wong H. K., Kurth W. S., Gurnett D. A., Granroth L. J., Groene J. B., 1996, Discrete, stimulated auroral kilometric radiation observed in the Galileo and DE 1 wideband data, *Journal of Geophysical Research*, 101, 10673

- Menietti J. D., Persoon A. M., Pickett J. S., Gurnett D. A., 2000, Statistical study of auroral kilometric radiation fine structure striations observed by Polar, *Journal of Geophysical Research*, *105*, 18,857
- Mutel R. L., Menietti J. D., Christopher I., 2004, AKR rain: A study of periodically modulated narrow-band drifting AKR emission observed with the Cluster WBD instrument, in *AGU Fall Meeting Abstracts*, pp SM23A-0496
- Mutel R. L., Menietti J. D., Christopher I. W., Gurnett D. A., Cook J. M., 2006, Striated auroral kilometric radiation emission: A remote tracer of ion solitary structures, *Journal of Geophysical Research*, *111*, A10203
- Mutel R. L., Peterson W. M., Jaeger T. R., Scudder J. D., 2007, Dependence of cyclotron maser instability growth rates on electron velocity distributions and perturbation by solitary waves, *Journal of Geophysical Research*, *112*, A07211
- Mutel R. L., Christopher I. W., Menietti J. D., Gurnett D. A., Pickett J. S., Masson A., Fazakerley A., Lucek E., 2011, RX and Z mode growth rates and propagation at cavity boundaries, in *Planetary, Solar and Heliospheric Radio Emissions (PRE VII)*, eds Rucker, H. O. and Kurth, W. S. and Louarn, P. and Fischer, G., pp 241-252
- Oya H., Morioka A., Kobayashi K., Lizima M., Ono T., 1990, Plasma wave observation and sounder experiments (PWS) using the Akebono (EXOS-D) satellite - Instrumentation and initial results including discovery of the high altitude equatorial plasma turbulence, *Journal of Geomagnetism and Geoelectricity*, *42*, 411
- Pottelette R., Treumann R. A., Berthomier M., 2001, Auroral plasma turbulence and the cause of auroral kilometric radiation fine structure, *Journal of Geophysical Research*, *106*, 8465
- Pritchett P. L., 1984, Relativistic dispersion, the cyclotron maser instability, and auroral kilometric radiation, *Journal of Geophysical Research*, *89*, 8957
- Santolík O., Parrot M., 2006, Propagation analysis of electromagnetic waves: Application to auroral kilometric radiation, *Lect. Notes Phys.*, *687*, 297
- Su Y.-J., Ma L., Ergun R. E., Pritchett P. L., Carlson C. W., 2008, Short-burst auroral radiations in Alfvénic acceleration regions: FAST observations, *Journal of Geophysical Research*, *113*, A08214
- Wu C. S., Lee L. C., 1979, A theory of the terrestrial kilometric radiation, *Astrophysical Journal*, *230*, 621